Applied Surface Science 302 (2014) 46–51

Contents lists available at ScienceDirect

Applied Surface Science

journal homepage: www.elsevier.com/locate/apsusc

# Double-beam pulsed laser deposition for the growth of Al-incorporated ZnO thin films

L. Moreno [a], C. Sánchez-Aké [a,*], M. Bizarro [b]

[a] Centro de Ciencias Aplicadas y Desarrollo Tecnológico, Universidad Nacional Autónoma de México, Circuito Exterior S/N, Ciudad Universitaria, AP 70-186, C.P. 04510 México D.F., México
[b] Instituto de Investigaciones en Materiales, Universidad Nacional Autónoma de México, Apartado Postal 70-186, C.P. 04510 México D.F., México

ARTICLE INFO

*Article history:*
Received 29 June 2013
Received in revised form
20 December 2013
Accepted 9 January 2014
Available online 7 February 2014

*Keywords:*
Double-beam pulsed laser deposition
Aluminum doped zinc oxide
Thin films
Plasma plume delay

ABSTRACT

Pulsed laser deposition in a delayed-double beam configuration is used to incorporate in situ Al in ZnO thin films. In this configuration, two synchronized pulsed-laser beams are employed to ablate independently a ZnO and an Al target. We investigated the effects of relative time delay of plasma plumes on the composition of the films with the aim of evaluating the performance of this technique to produce doped materials. Relative delay between plumes was found to control the incorporation of Al in the film in the range from 14% to 30%. However, to produce low impurity concentration of Al-doped ZnO (with Al incorporation less than 2%) the fluence used to produce the plasmas has more influence over the film composition than the relative plume delay. The minimum incorporation of Al corresponded to a relative delay of 0 μs, due to the interaction between plumes during their expansion.



## Introduction

Pulsed laser deposition (PLD) has been employed to grow thin films of a great diversity of materials including polymers, semiconductors, metals and even biological materials. Its main advantages in comparison with other deposition techniques are the high growth rate, lack of harmful precursor chemicals, stoichiometric transfer and that it can be applied to essentially any material [1]. A disadvantage of conventional PLD (as in other physical methods for films deposition), is the necessity to prepare new targets of specific compositions in order to produce films with different compositions. This drawback has been addressed using alternative configurations that involve multiple targets and laser beams. In the case of two different targets ablated simultaneously, the ejected materials can be mixed directly in the colliding plumes resulting in films of binary or ternary compounds [1,2]. Moreover, the interaction between plasma plumes can enhance the nonequilibrium nature of PLD, affecting the limit of solubility of materials or resulting in the formation of abnormal metastable structures or new ordered intermetallic phases [1].

Multi-laser and multi-target PLD has already been employed to produce thin films of complex compositions specially designed for particular applications [3,4]. However, the composition of the film depends on several experimental parameters, which must be optimized to produce high quality materials. Two parameters that play an important role in the interaction between plasma plumes and therefore in the composition of the films are: the laser fluence and the relative time delay between plumes. Both parameters can be modified during the growing stage making it possible to modify the composition of the film in situ. The relative delay between plumes dictates the kind of interaction between plasmas and also affects the relative arrival time of the plume components to the substrate. Despite its importance, there are only few reports in which the influence of this parameter on the deposited films has been studied, and some results are contradictory. For example, Hussey et al. [5] found that the quality of YBCO films was independent of the delay between pulses. Sloyan et al. [3] found that the relative time delay between plumes on thin garnet crystal films affect both the lattice constant and elemental composition of the films. We previously found [6] that by changing the relative delay between plasma plumes it is possible to modify the dopant incorporation in Mn-doped ZnO films. The reason for the diversity of these results is that the interaction between plasmas depends on several parameters such as: laser fluence, the material from which the target is made, the background pressure during the film growth, among others.

Here we study the influence of the relative time delay between plumes in double-beam PLD on the incorporation of Al into ZnO films. We chose this material since it has been exhaustively characterized and its structural, electrical and optical properties are well

* Corresponding author. Tel.: +52 5556228602x1217.
*E-mail addresses:* citlali.sanchez@ccadet.unam.mx, cit-ake@unam.mx (C. Sánchez-Aké).

0169-4332/$ – see front matter © 2014 Elsevier B.V. All rights reserved.
http://dx.doi.org/10.1016/j.apsusc.2014.01.051

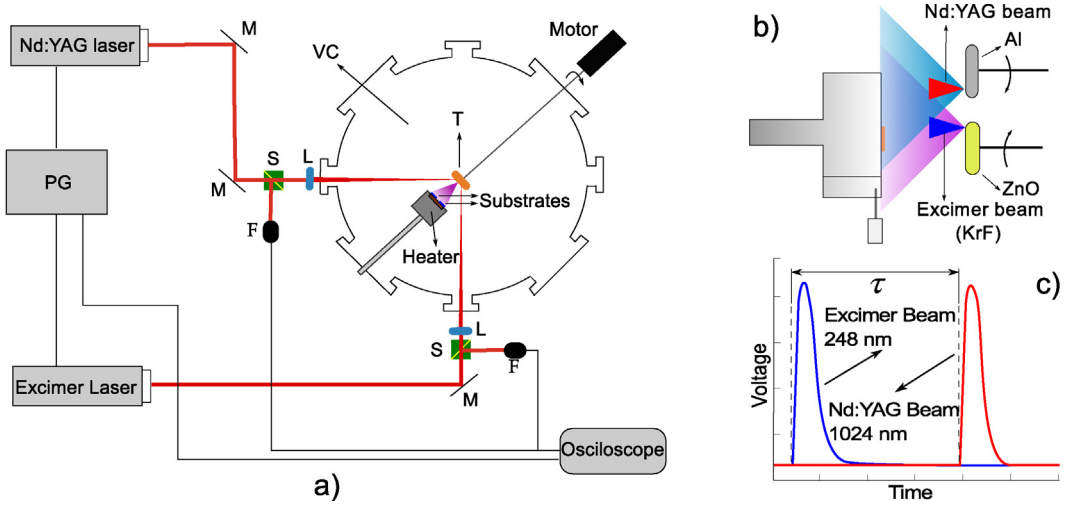


**Fig. 1.** (a) View from above of the experimental setup: PG: pulse delay generator, M: mirror, S: beam splitter, L: lens, F: photodiode, T: target, VC: vacuum chamber, (b) lateral view of the target arrangement; left: heater over which the substrates are located, right: ablated targets, (c) oscilloscope signal of the temporal delay ($\tau$) between laser beams.

known. The experiments were performed using different laser fluences with the aim to evaluate the potential of this technique to produce doped thin films.

## Experimental setup

Fig. 1 shows a schematic diagram of the experimental configuration. Two lasers were used: a Nd:YAG (1064 nm, pulse duration: 7 ns repetition rate: 10 Hz) and an Excimer KrF (248 nm, pulse duration: 30 ns repetition rate: 10 Hz). Both laser beams were directed to a vacuum chamber using a set of mirrors until their arrival to their respective plane-convex lens that focuses the beam to their respective targets. The excimer laser beam was focused onto a 1-inch-diameter ZnO target while the Nd:YAG laser impinges on a 1-inch-diameter Al target. The ZnO target was located below the Al target with a separation of 1 mm and the distance between the laser spots was 1.6 cm (Fig. 1b). Two types of substrates were used: Corning glass and silicon wafers (100). The substrates were located right next to each other at a distance normal to the targets of 4.5 cm. With this disposition, both substrates were reached by the overlapping plumes during the deposition of the films. Two different sets of films were grown under different experimental conditions in order to evaluate the effect of the delay between pulses on the composition of the films. Table 1 shows the used fluence for both sets as well as other relevant deposition parameters. The Nd:YAG laser fluence was changed between both sets to affect the amount of Al extracted from the target and therefore its incorporation in the film. For the case of the ZnO target, we kept fixed the fluence of the excimer laser, but changed the values of the energy and spot size. These parameters affect the density of the plasma and the energy of the species in the expanding plume. In this way, we evaluate the influence of those parameters on the interaction between plasmas for different delays between plumes. The delay between laser pulses ($\tau$) was controlled by means of a pulse delay generator. The used temporal differences were: 0, 5, 10, 100 and 1000 μs. The first emitted beam always corresponded to the excimer laser.

The films were deposited at a constant temperature of 400 °C. A 1 mTorr $O_2$ atmosphere was established in the chamber after a pressure of $1 \times 10^{-6}$ Torr has been achieved. The Al content in the doped ZnO films was measured using energy dispersive x-ray spectroscopy (EDS, JSM-7600F, Jeol) and the crystalline structure was analyzed by x-ray diffraction (D8 Advance Bruker) using the Cu $K\alpha_1$ wavelength (1.54056 Å). The resistivity of the films was determined by the four-point probe technique. The transmittance of the films was measured using an Analytical Instrument Systems light source model DT-1000CE-S and an Ocean Optics fiber optic spectrometer model USB2000. EDS and Resistivity were measured on the silicon wafer substrate, while XRD and transmittance were measured on the corning glass substrate.

## Results and discussion

Fig. 2a and b show the XRD results of sets 1 and 2, respectively. In both sets, the ZnO films grown by conventional PLD using a single target (black line) show the (0 0 2) and (0 0 4) peaks of the wurtzite structure [7,8]. These films were deposited using the same laser fluence, nevertheless the values of the laser energy and the spot size were different (see Table 1). Both variables affect important physical parameters of the plume, which in turn affect the properties of the deposited film. For example, the laser energy can affect the kinetic energy of the species and the composition of the plume, meanwhile the spot size can modify the amount of ablated material and the volume of the plume. It has been shown that the O/Zn and ionized/neutral flux ratios affect the crystallinity and morphology of the films [9,10] and that the kinetic energy of the species reaching the substrate affects the structure and stress in the film [11]. Here we used two conditions of the same fluence in which the deposited films have similar crystalline structure, transparency and bandgap (shown below). We chose these conditions to study the influence of

**Table 1**
Energy, spot area and used fluence for the two deposited set of films. Deposition conditions: deposition time: 30 min, repetition rate: 10 Hz.

| | Excimer laser | | | Nd:YAG | | |
|---|---|---|---|---|---|---|
| | Laser energy (mJ) | Area ($cm^2$) | Fluence ($J/cm^2$) | Laser energy (mJ) | Area ($cm^2$) | Fluence ($J/cm^2$) |
| Set 1 | $60 \pm 6$ | $0.020 \pm 6 \times 10^{-4}$ | $3.0 \pm 0.4$ | $60 \pm 6$ | $0.010 \pm 6 \times 10^{-4}$ | $6.0 \pm 1$ |
| Set 2 | $23 \pm 2.3$ | $7 \times 10^{-3} \pm 6 \times 10^{-4}$ | $3.0 \pm 0.6$ | $2.5 \pm 0.25$ | $4 \times 10^{-3} \pm 6 \times 10^{-4}$ | $0.6 \pm 0.2$ |

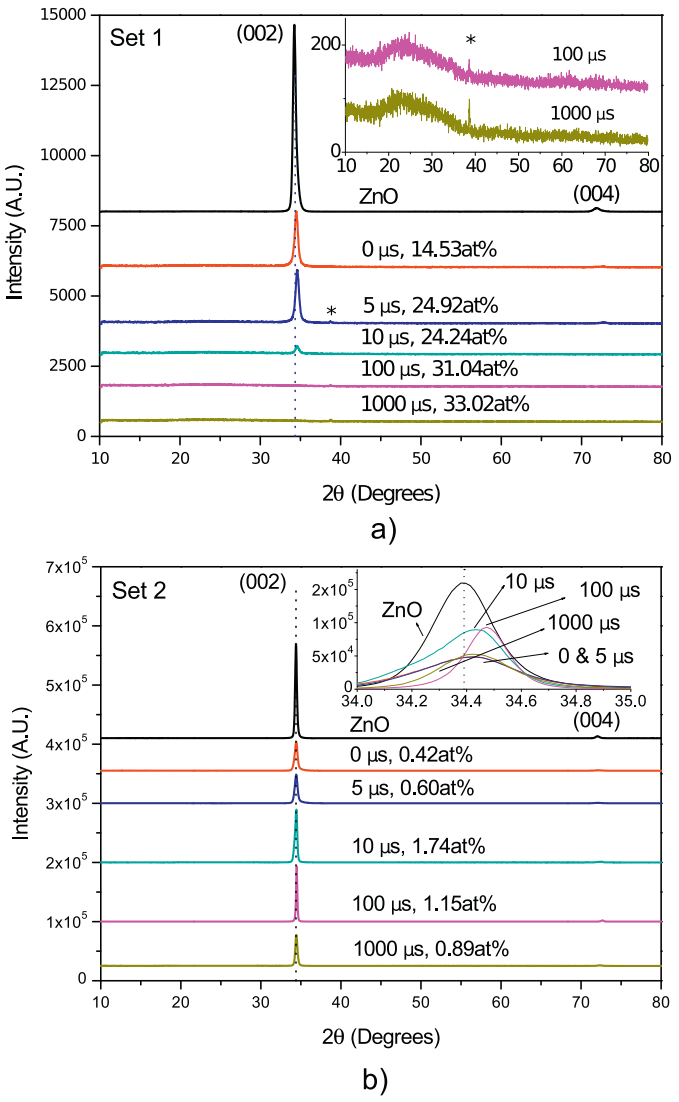


**Fig. 2.** XRD results of the set of films grown with a Nd:YAG fluence of (a) 6 J/cm$^2$ and (b) 0.6 J/cm$^2$. Inset (a) zoom of the diffraction spectra for the films grown at $\tau = 100$ µs and $\tau = 1000$ µs. Inset (b) zoom of the (0 0 2) peak. The dotted line in both graphs represents the center of the (0 0 2) peak of the undoped ZnO film. In (a) the intensity of the diffraction data of the undoped ZnO film was decreased by a factor of 10, while in (b) the data corresponding to the film grown at $\tau = 100$ µs was decreased by a factor of three.

the delay between plumes in double-beam PLD since the ZnO plasmas are different although the films have similar characteristics. For the case of set 1 (see Fig. 2a), the films grown using double-beam PLD show a decrement in the intensity of the (0 0 2) and (0 0 4) peaks with the increase of the delay between plumes indicating a loss of crystallinity [8,12]. Furthermore, both diffraction peaks show a shift towards greater angles with increasing $\tau$, and disappear for $\tau > 10$ µs. This result indicates an increment of the Al content with $\tau$ and is consistent with the EDS results shown below. The shift of the (0 0 2) peak has been reported before for ranges of 1% to 6% of Al doping of films deposited on silicon, glass and quartz substrates [8,12,13], and it has been associated with a residual stress parallel to the *c*-axis of the wurtzite structure and the substitution of $Zn^{2+}$ with $Al^{3+}$. As the ionic radius of $Al^{3+}$ is smaller than that of $Zn^{2+}$, the value of the *c*-axis is expected to decrease, therefore causing the peaks to shift towards greater angles. Those results strongly suggest that for $\tau \leq 10$ µs the incorporation of Al in the films is substitutional. In contrast, the films grown at $\tau = 100$ and 1000 µs do not present diffraction peaks corresponding to ZnO while there is presence of a diffraction peak around 38.6° (also present for $\tau = 5$ µs). This indicates the presence of a second phase, which could be associated to the (1 1 0) planes of $Al_2O_3$ [14]. The presence of $Al_2O_3$ peaks has been reported before in Al-doped ZnO films for doping percentages of 30% [8], indicating that the films grown with $\tau = 100$ and 1000 µs have larger amount of Al than those for $\tau \leq 10$ µs.

Fig. 2b shows the XRD results for the second set of samples. For this group, all the films maintained the wurtzite structure crystalline structure, presenting the (0 0 2) and the (0 0 4) peaks. The presence of both peaks in all films indicates that a lesser amount of Al has been incorporated in comparison with that of set of Fig. 2a. This result was expected as the first set was grown at a greater laser fluence (for the Al target) than the second set. The diffraction peaks have a shift towards greater angles, suggesting again that the incorporation of Al is substitutional. In particular, the film corresponding to a delay of $\tau = 100$ µs shows the greatest shift and intensity among all the samples. In regard to the former, this can be the result of a greater stress inside the film in comparison to the rest of the samples, while the latter suggests a better crystalline structure within the film. The XRD results show that the effect of $\tau$ and the used fluence are different in both sets. The crystalline structure of the films of set 2 remained constant while the films of set 1 showed noticeable changes, indicating important modifications in their composition.

Fig. 3a and b show the EDS results as a function of the delay between laser pulses of the set 1 and the set 2, respectively. Fig. 3a shows that the film deposited at $\tau = 0$ µs has the smallest content of Al (blue dotted line) and the maximum incorporation of Zn (red dotted line). As $\tau$ increases, the presence of Al in the film increases while the presence of Zn diminishes. The oxygen content oscillates around a constant value except for the film grown at $\tau = 100$ µs. The decrement of Zn and increase of Al content for delays $\leq 10$ µs suggests that Al replaces Zn in the film. This result agrees with the shift towards larger angles of the peaks (0 0 2) and (0 0 4) observed in the XRD spectra (see Fig. 2a). In contrast, for values of $\tau \geq 100$ µs the amount of Al and Zn remain practically constant and the only differences in the film composition correspond to that of O. Those films have an incorporation of Al about 30%, which explains the presence of the $Al_2O_3$ peak observed in Fig. 2a. The changes in the amount of incorporated Al as function of $\tau$ in this set, agree with those previously reported for Mn-doped ZnO films [6]. In that work it was found that the influence of $\tau$ on the composition of the films was due to the interaction between plasma plumes. Such interaction takes place in two different regimes depending on $\tau$ [3,6]. For values of $\tau \sim 10$ µs or smaller, an overlapping of the plumes causes scattering of lighter cations from the plumes. For the case of delays of about few hundreds of µs, the first plume expands through the background gas and lefts behind a partial vacuum, which affects the expansion of the second plume. In the case of Fig. 3a, for $\tau \leq 10$ µs, the interaction between plasma plumes causes the atoms and ions that compose the Al plasma to deflect from their original trajectory [6], eventually causing less incorporation of Al in the deposited films. For $\tau \sim 100$ µs, the interaction between plumes is not collisional, because when the second plume is produced, the species of the ZnO plasma have already reached the substrate. Nevertheless, a slight increase in the amount of O was observed. This result is unexpected and probably is due to the formation of a second phase ($Al_2O_3$), which in turn is caused by the high content of Al (larger than 30%) and might be influenced by the expansion of the Al plume through a partial vacuum created by the propagation of the earlier plume [3]. Finally for $\tau \geq 1000$ µs, the interaction between plasmas is practically negligible, therefore the Al plume can reach the substrate such as in conventional PLD.

Fig. 3b shows the EDS results for the second set of films. A tendency of the Zn to decrease with increasing delay $\tau$ is observed, until $\tau = 100$ µs where the behavior of Zn in the films does not show

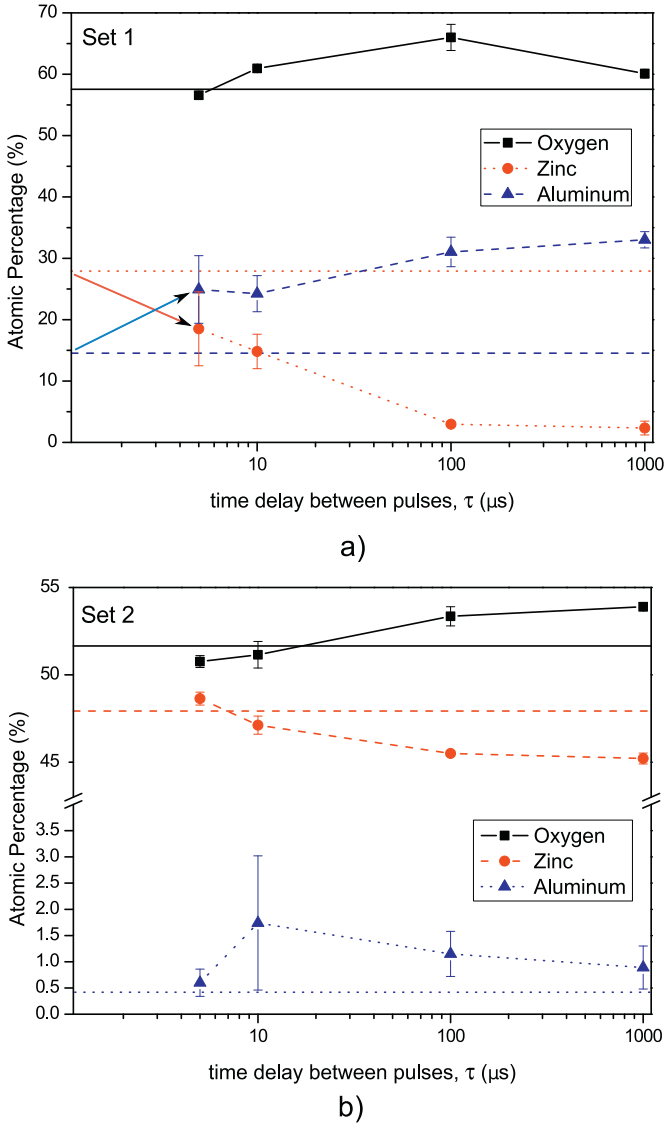


**Fig. 3.** Chemical composition of the set of films grown with a Nd:YAG (Al target) energy of a) 60 mJ (fluence: 6 J/cm$^2$) and (b) 2.5 mJ (fluence: 0.6 J/cm$^2$). The horizontal lines represent the chemical composition of the films grown at $\tau = 0$ μs.

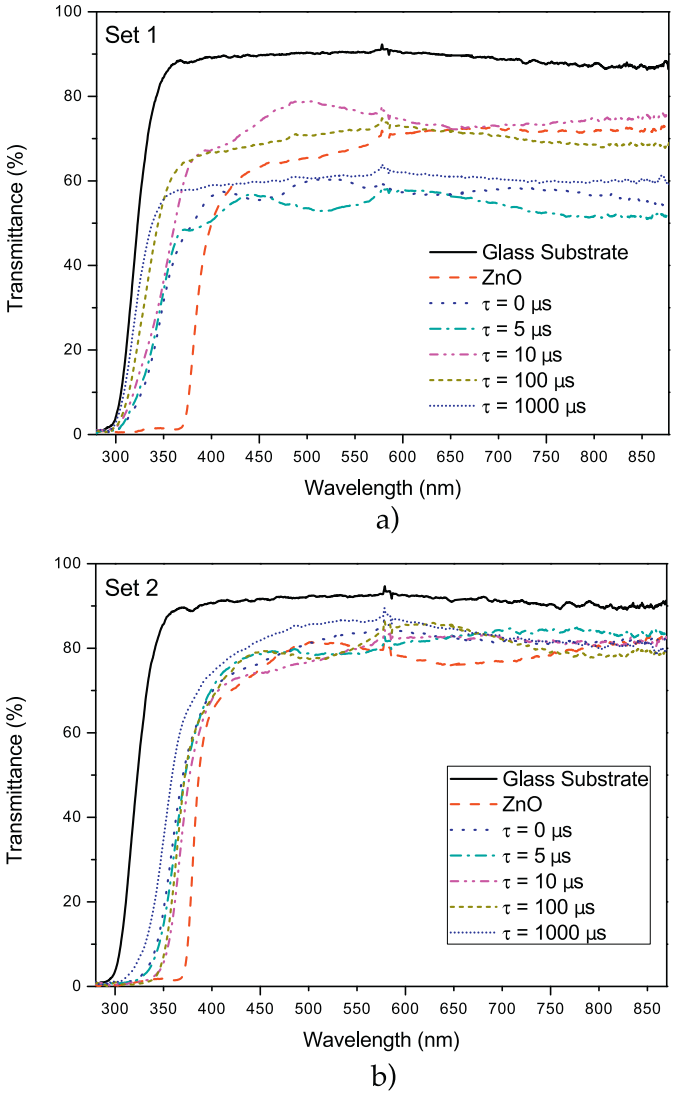


**Fig. 4.** Transmittance of the set of films grown with a Nd:YAG fluence of (a) 6 J/cm$^2$ and (b) 0.6 J/cm$^2$.

significant variation. The O seems to increase its presence as the delay between laser pulses increases, passing through a minimum at $\tau = 5$ μs. As in set 1, the film deposited at $\tau = 0$ μs has the smallest content of Al (blue dotted line). For larger delays the amount of Al in the films varies between values from 0.42% to 1.74% and shows no clear tendency in relationship with $\tau$· For $\tau \geq 10$ μs the content of Al can even be considered constant taking into account the error bars, which correspond to the standard deviation calculated with the measurements in different regions of the films. Also, due to the behavior of oxygen in this set of films, the substitution of Al for Zn does not have a clear behavior as the one found for the first set of films. However, Hong et al. [15] found that for Al-doped ZnO films there is no clear relationship between the presence of Al and O in the films, while showing a decrease in the presence of Zn with a rapid increase of Al concentration. This suggests that even though the O in the films appears to be increasing with respect to $\tau$, the substitution of $Zn^{2+}$ for $Al^{3+}$ may still be taking place.

The variation in the amount of Al between both sets is due to the utilized fluence to ablate the Al target, which was lower for the set 2. This caused a smaller extraction of material and consequently the presence of Al in the films was diminished in comparison to that found in the first set. However, for both sets the lesser amount of Al in the films was found for simultaneous pulses. This suggests that for both sets there exists a similar underlying physical process taking place at $\tau = 0$ μs that minimize the incorporation of Al in the films. The nature of the physical processes that occur during the plasmas expansion was not studied in this work. However, according to a previous work [6], for simultaneous pulses there exists a larger deviation of the plasma plumes before reaching the substrate, which can decrease the Al in the films.

For greater delays the Al incorporation increased in both sets. However, the properties of the films and their incorporation of Al changed with the use of different conditions. For set 1, a clear increasing substitution of $Zn^{2+}$ for $Al^{3+}$ with increasing time delay was observed. However for set 2 such clear behavior was not present. This shows that laser fluence is a critical factor for precisely controlling the amount of Al present in the films and that there exist physical processes within the plasma plumes that affect the dopant quantity, which in turn, also modify the structure and properties of the films.

Fig. 4a shows the transmittance spectra of the first group of films. The mean transmittance of this group was (73.00 ± 9.45)%. The spectra can be directly compared with exception of that for the

**Table 2**
Bandgap and thickness of the films of set 1 and set 2. The resistivity for set 2 is also shown.

| | Set 1 | | Set 2 | | |
|---|---|---|---|---|---|
| | Bandgap (eV) | Thickness (nm) | Bandgap (eV) | Thickness (nm) | Resistance (Ω cm) |
| ZnO | 3.27 | 189.3 ± 69.0 | 3.28 | 91.6 ± 29.4 | $3.78 \times 10^{-2} \pm 9.03 \times 10^{-4}$ |
| $\tau = 0$ μs | 3.69 | 402.4 ± 51.5 | 3.55 | 69.5 ± 36.9 | $5.84 \times 10^{-4} \pm 1.23 \times 10^{-5}$ |
| $\tau = 5$ μs | 3.85 | 173.6 ± 10.6 | 3.50 | 68.2 ± 14.9 | $8.00 \times 10^{-4} \pm 4.64 \times 10^{-5}$ |
| $\tau = 10$ μs | 3.86 | 169.6 ± 36.2 | 3.41 | 43.6 ± 2.1 | $7.64 \times 10^{-4} \pm 2.38 \times 10^{-5}$ |
| $\tau = 100$ μs | 3.97 | 174.6 ± 71.6 | 3.49 | 159.5 ± 10.4 | $4.85 \times 10^{-4} \pm 1.37 \times 10^{-5}$ |
| $\tau = 1000$ μs | 4.01 | 176.8 ± 8.6 | 3.73 | 123.2 ± 71.6 | $6.37 \times 10^{-4} \pm 3.51 \times 10^{-5}$ |

film grown with $\tau = 0$, since its thickness was considerable larger than that of the rest of the group (see Table 2). That film was grown under the condition of maximum overlapping between plumes. The physical mechanisms for which this film was the thickest of set 1 were not determined. However, a possible explanation is that the collision between plumes decreases the species kinetic energy avoiding the sputtering of the deposited film.

The absorption coefficient ($\alpha$) was determined using the transmission spectra, in order to analyze the optical band gap of the films. Considering that ZnO is a direct transition semiconductor, $(\alpha h\upsilon)^2$ against the photon energy $h\upsilon$ was plotted. The extrapolation of the linear part of the curve to zero gives the value of $E_g$, which showed a blue-shift as the Al percentage increased for the films of set 1 (Table 2). This could be mainly due to the Burstein-Moss shift since the incorporation of Al in the films is in the range from 14% to 30%. This effect states that the introduction of impurities may fill states at the bottom of the conduction band. As the Pauli's exclusion principle forbids a double occupied state and the optical transitions are vertical, the electrons in the valence band require higher energy to be excited to the states in the conduction band producing a blue-shift of $E_g$ [16]. However, other factors can be responsible for it, such as a stress present inside the film, which agrees with the shift of the diffraction peaks in the XRD results and also variations in the density of impurities caused by the change in the crystalline structure [17,18].

Fig. 4b shows the results obtained for the transmittance of the second set of films. The mean transmittance was (89.57 ± 0.35)%. The thickness and the values of the optical band gap are shown in Table 2. The deposition rate, and therefore the thickness of the films of set 2 was smaller than that for the set 1 due to the differences of the used fluences between both sets. For set 2, the Nd:YAG laser fluence was an order of magnitude smaller than that for set 1. The excimer laser energy and the spot size were also small for set 2, producing less ablated material and therefore a lower deposition rate. In this set, the thickness of the films depends on the delay between plasmas. The films grown with $\tau = 0$, 5 and 10 μs had the smallest thickness, suggesting that there is an interaction between plasmas. Further experiments should be performed to determine the nature of that interaction and its effect on the thickness of the films. The absorption edge of the films in this set presents anew a shift towards lower wavelengths in comparison to the ZnO film, but the shift is smaller than in set 1. This could be attributed to the lower impurity level present in the Al-doped films as well as the increase of O within them. Also, the band gap values do not show a uniform trend as that measured in Set 1. This could be attributed to the lack of uniformity of the Al inside the films, as showed in the error bars in the EDS results. Another reason might be the differences between films thickness, where it has been shown that for values smaller than 100 nm, the thickness of ZnO:Al films heavily influences the bandgap value [19].

Comparing both sets, the films grown with the greater fluence (set 1) showed a lesser transparency to that grown with the smaller fluence (set 2). This is attributed to the Al difference between both sets. The shift towards lower wavelengths of the absorption edge observed in both sets might be caused not only by the Burstein-Moss shift, but also due to stress, variation of impurities within the film and the film thickness.

The resistivity was measured only for the films of second set since the presence of second phases was not observed. The undoped ZnO film was measured to be $3.78 \times 10^{-2}$ Ω cm whereas the resistivity of the doped films oscillates around $6.5 \times 10^{-4}$ Ω cm (Table 2). A minimum was obtained at $\tau = 100$ μs of $4.85 \times 10^{-4}$ Ω cm which corresponds to a dopant percentage of 1.15%. These results show that for set 2 there is not an evident trend between the resistivity and $\tau$· A decrease in resistivity in the range (0–1.5)% of Al doping has been previously observed [20]; such resistivity values increase for greater Al doping percentages. The diminishing in resistivity of Al:ZnO films has been associated with the substitution of $Zn^{2+}$ by $Al^{3+}$ [21], fact that is strongly suggested in our films by the XRD results previously presented. It has also been reported that films highly oriented along the *c*-axis, exhibit a decrease in resistivity [22] and it has been demonstrated that the film resistivity is inversely proportional to the degree of (0 0 2) orientation of doped ZnO films [23]. These findings coincide with our results, were the minimum resistivity was found for $\tau = 100$ μs, film that corresponds to the greatest *c*-axis orientation according to the XRD results.

## Conclusions

The delayed double-beam pulsed laser deposition technique has proved to be useful to incorporate Al in ZnO films in situ. The results presented showed two different effects of $\tau$ on the composition and structure of the films. For the conditions used in set 1, the delay between plumes modified the amount of Al in the films in a wide range (approximately from 14% to 30%). On the contrary, the films of set 2 had incorporation of Al <2% and did not show a clear tendency with $\tau$. Our results showed that the composition of the films depends on the delay between plumes as well as of the utilized fluence of the incident laser beams. Moreover it was shown that the laser fluence is a critical factor on the effect of the delay between plumes and therefore in the properties of the films, which explains the contradictory results found in the literature. This study demonstrates that for the adequate experimental conditions, delayed double-beam PLD is a useful approach to incorporate large amounts Al in ZnO films in situ. Therefore it provides a method to produce films with gradients in composition of different materials. However, for incorporation of low amounts of Al in ZnO (doped films), the fluence to produce the plasmas plays a more important role than the relative plume delay. The results found in this work could be extended to other materials to produce binary/ternary compounds or doped thin films. However, further investigations should be performed to relate the physical properties of the plasmas with their interaction to improve the performance of delayed double-beam PLD.

## Acknowledgments

This work was funded by the CONACyT under grant number 82634 and the DGAPA-UNAM under grants IN110612 and

IB101912-RR181912. The authors would like to acknowledge to A. Tejeda and O. Novelo for their collaboration on this work.

## References

[1] R.W. Eason (Ed.), Pulsed Laser Deposition of Thin Films: Applications-Led Growth of Functional Materials, John Wiley & Sons, Inc., Hoboken, NJ, 2007.
[2] L. Escobar-Alarcón, J. Pérez-Álvarez, D. Solís-Casados, E. Camps, S. Romero, J. Jiménez-Becerril, Appl. Phys. A 110 (2013) 909.
[3] K.A. Sloyan, T.C. May-Smith, R.W. Eason, J.G. Lunney, Appl. Surf. Sci. 255 (2009) 9066.
[4] T.C. May-Smith, K.A. Sloyan, R. Gazia, R.W. Eason, Cryst. Growth Des. 11 (2011) 1098.
[5] B.W. Hussey, A. Gupta, J. Appl. Phys. 72 (1992) 287.
[6] C. Sánchez-Aké, R. Camacho, L. Moreno, J. Appl. Phys. 112 (2012) 044904.
[7] K.H. Kim, K.C. Park, D.Y. Ma, J. Appl. Phys. 81 (1997) 7764.
[8] J.G. Lu, Z.Z. Ye, Y.J. Zeng, L.P. Zhu, L. Wang, J. Yuan, B.H. Zhao, Q.L. Liang, J. Appl. Phys. 100 (2006) 073714.
[9] A. Klini, A. Manousaki, D. Anglos, C. Fotakis, J. Appl. Phys. 98 (2005) 123301.
[10] T. Nakamura, K. Masuko, A. Ashida, T. Yoshimura, N. Fujimura, Thin Solid Films 518 (2010) 2971.
[11] J. Perrière, E. Millon, W. Seiler, C. Boulmer-Leborgne, V. Craciun, J. Appl. Phys. 91 (2002) 690.
[12] S. Venkatachalam, Y. Iida, Y. Kanno, Superlattices Microstruct. 44 (1) (2008) 127.
[13] Y. Liu, Q. Li, H. Shao, J. Alloys Compd. 485 (1–2) (2009) 529.
[14] JCPDS-International Centre for Diffraction Data 46-1212, 1998.
[15] R.J. Hong, X. Jiang, B. Szyszka, V. Sittinger, A. Pflug, Appl. Surf. Sci. 207 (2003) 341.
[16] B.E. Sernelius, K.-F. Berggren, Z.-C. Jin, I. Hamberg, C.G. Granqvist, Phys. Rev. B: Condens. Matter 37 (1988) 10244–10248.
[17] M. Suchea, S. Christoulakis, M. Katharakis, N. Vidakis, E. Koudoumas, Thin Solid Films 517 (15) (2009) 4303.
[18] M. Bizarro, A. Sánchez-Arzate, I. Garduño-Wilches, J.C. Alonso, A. Ortiz, Catal. Today 166 (2011) 129.
[19] B.Z. Dong, G.J. Fang, J.F. Wang, W.J. Guan, X.Z. Zhao, J. Appl. Phys. 101 (2007) 033713.
[20] X. Zi-qiang, D. Hong, L. Yan, C. Hang, Mater. Sci. Semicond. Process. 9 (1–3) (2006) 132.
[21] R.K. Shukla, Anchal Srivastava, Atul Srivastava, K.C. Dubey, J. Cryst. Growth 294 (2006) 427.
[22] N.P. Dasgupta, S. Neubert, W. Lee, O. Trejo, J. Lee, F.B. Prinz, Chem. Mater. 22 (2010) 4769.
[23] J. Lee, B. Park, Thin Solid Films 426 (2003) 94.